A NUMERICAL STUDY OF THE INTERACTION BETWEEN ELASTIC AND VISCOUS EFFECTS IN MAXWELL-B FLUID FLOWS

Cleiton Fonseca, cfonseca@mecanica.ufrgs.br
Sergio L. Frey, frey@mecanica.ufrgs.br
Laboratory of Applied and Computational Fluid Mechanics (LAMAC), Department of Mechanical Engineering
Federal University of Rio Grande do Sul, Rua Sarmento Leite 425, RS 90050-170, Brazil

Mônica F. Naccache, naccache@puc-rio.br
Department of Mechanical Engineering, Pontifícia Universidade Católica do Rio de Janeiro
Rua Marquês de São Vicente 225, RJ 22453-900, Brazil

Abstract. *The goal of this work is to perform finite element approximations for creeping flows of nonlinear viscoelastic fluids. For this end, a Galerkin least-squares formulation, in terms of extra-stress, pressure and velocity, is employed. Its major features are to remain stable even in elastic-dominated flow regions and to allow the use of a combination of equal-order bilinear finite element interpolations. Some numerical simulations of steady creeping flows of Maxwell-B fluids around a cylinder kept inside a planar channel are performed, aiming the investigation of the elastic influence on viscoelastic fluid dynamics.*

Keywords*: Viscoelastic fluids, upper-convected Maxwell-B model, multi-field Galerkin least-squares method*

1. INTRODUCTION

Viscoelastic flows are found in several industrial applications, such as oil recovery, paper and textile coating and extrusion of polymeric materials. Numerical simulations are usually employed to study industrial processes using viscoelastic fluids, since experiments can be very expensive and time consuming (Owens and Phillips, 2002).

The present work performs multi-field Galerkin least-squares (GLS) approximations in terms of extra-stress, pressure and velocity fields (Behr et al., 2004), for non-linear differential viscoelastic flows, using the upper convected Maxwell model (Astarita and Marrucci, 1974). The multi-field approximation for such model consists on a variational formulation for the momentum and mass balance equations, coupled with an extra-stress-rate-type constitutive equation. An additional difficulty arises from the multi-field approximation, when compared to mixed approximations, namely, the handling of the extra-stress tensor as a primal variable. In the finite element context, two compatibility conditions appear for such a model: the need to satisfy the classical Babuška-Brezzi condition involving finite element sub-spaces for velocity and pressure fields, and a second compatibility condition between extra-stress and velocity finite element subspaces (Behr et al., 1993),. This formulation is developed as an attempt to enhance the stability of the classical Galerkin approximation for differential viscoelastic flows, which major feature is to circumvent the compatibility conditions between velocity-pressure and extra-stress-velocity finite sub-spaces, hence allowing the use of simple combinations of finite element interpolations, as the equal-order bi-linear one. Furthermore, due to an appropriate design of its least-squares mesh-dependent terms, this formulation remains stable even for locally elastic-dominated flows, wherein the upper-convected derivative of the material equation plays a relevant role (Franca and frey, 1992).

To evaluate the performance of the GLS formulation, we use the benchmark problem of the steady creeping flow through a cylinder inside a planar channel. Moreover, we determine the elasticity effect on the flow field and stress components through the variation of the Deborah number from 0 to 0.9.

2. MODELING

A multi-field boundary-value problem for steady creeping flows of upper-convected Maxwell fluids may be stated coupling the continuity and momentum equations with the UCM viscoelastic equation (Astarita and Marrucci, 1974), subjected to appropriate velocity and stress boundary conditions,

$$\begin{aligned}
&\operatorname{div}\boldsymbol{\tau} - \nabla p + \rho\,\mathbf{b} = \mathbf{0} && \text{in } \Omega \\
&\boldsymbol{\tau} + \lambda \overset{\nabla}{\boldsymbol{\tau}} = 2\eta_p \mathbf{D}(\mathbf{u}) && \text{in } \Omega \\
&\operatorname{div}\mathbf{u} = 0 && \text{in } \Omega \\
&\mathbf{u} = \mathbf{u}_g && \text{on } \Gamma_g^{\mathbf{u}} \\
&\boldsymbol{\tau} = \boldsymbol{\tau}_g && \text{on } \Gamma_g^{\boldsymbol{\tau}} \\
&(\boldsymbol{\tau} - p\mathbf{1})\,\mathbf{n} = \mathbf{t}_h && \text{on } \Gamma_h
\end{aligned} \tag{1}$$

where the open bounded set $\Omega \subset \Re^2$, with a regular polygonal boundary Γ, denotes the fluid domain, the velocity vector $\mathbf{u}$, the hydrostatic pressure p, and the extra-stress tensor $\boldsymbol{\tau}$, are the primal variables of Eq. (1), ρ is the fluid density, λ is the fluid relaxation time, η_p, is the polymeric viscosity, $\mathbf{D}$ is the strain rate tensor, $\mathbf{b}$ is the body force per unit of mass, $\mathbf{t}_h$ is the stress vector, $\mathbf{u}_g$ and $\boldsymbol{\tau}_g$ are the imposed velocity and extra-stress boundary conditions, respectively. Furthermore, the upper-convected time derivative of $\boldsymbol{\tau}$ is defined by

$$\check{\boldsymbol{\tau}} = (\nabla \boldsymbol{\tau})\mathbf{u} - (\nabla \mathbf{u})\boldsymbol{\tau} - \boldsymbol{\tau}(\nabla \mathbf{u})^T \tag{2}$$

2.1. A multi-field GLS formulation

A multi-field GLS formulation for upper-convected Maxwell fluid flows governed by Eq.(1)-(2) may be written as: *find the triple* $(\boldsymbol{\tau}^h, p^h, \mathbf{u}^h) \in \boldsymbol{\Sigma}^h \times P^h \times \mathbf{V}_g^h$ *such as:*

$$B(\boldsymbol{\tau}^h, p^h, \mathbf{u}^h; \mathbf{S}^h, q^h, \mathbf{v}^h) = F(\mathbf{S}^h, q^h, \mathbf{v}^h) \quad \forall (\mathbf{S}^h, q^h, \mathbf{v}^h) \in \boldsymbol{\Sigma}^h \times P^h \times \mathbf{V}_g^h \tag{3}$$

where

$$\begin{aligned} B(\boldsymbol{\tau}^h, p^h, \mathbf{u}^h; \mathbf{S}^h, q^h, \mathbf{v}^h) &= (2\eta_p)^{-1} \int_\Omega \boldsymbol{\tau}^h \cdot \mathbf{S}^h \, d\Omega - \int_\Omega \mathbf{D}(\mathbf{u}^h) \cdot \mathbf{S}^h \, d\Omega + \int_\Omega \boldsymbol{\tau} \cdot \mathbf{D}(\mathbf{v}^h) \, d\Omega \\ &+ (2\eta_p)^{-1} \int_\Omega \lambda ((\nabla \boldsymbol{\tau}^h)\mathbf{u}^h - \nabla \mathbf{u}^h \boldsymbol{\tau}^h - \boldsymbol{\tau}^h \nabla (\mathbf{u}^h)^T) \cdot \mathbf{S}^h \, d\Omega - \int_\Omega p^h \operatorname{div} \mathbf{v}^h \, d\Omega + \int_\Omega \operatorname{div} \mathbf{u}^h q^h \, d\Omega \\ &+ \epsilon \int_\Omega p^h q^h \, d\Omega + \alpha \sum_{K \in \Omega^h} \int_{\Omega_K} (\nabla p^h - \operatorname{div} \boldsymbol{\tau}^h) \cdot (\nabla q^h - \operatorname{div} \mathbf{S}^h) \, d\Omega \\ &+ 2\eta_p \int_\Omega ((2\eta_p)^{-1} \boldsymbol{\tau}^h + (2\eta_p)^{-1} \lambda ((\nabla \boldsymbol{\tau}^h)\mathbf{u}^h - \nabla \mathbf{u}^h \boldsymbol{\tau}^h - \boldsymbol{\tau}^h \nabla (\mathbf{u}^h)^T) - \mathbf{D}(\mathbf{u})^h) \cdot \\ &\qquad \cdot \beta(\mathrm{De}_K)((2\eta_p)^{-1} \mathbf{S}^h + (2\eta_p)^{-1} \lambda ((\nabla \mathbf{S}^h)\mathbf{u}^h - \nabla \mathbf{u}^h \mathbf{S}^h - \mathbf{S}^h \nabla (\mathbf{u}^h)^T) - \mathbf{D}(\mathbf{v})^h) \, d\Omega \end{aligned} \tag{4}$$

and

$$F(\mathbf{S}^h, q^h, \mathbf{v}^h) = \int_\Omega \rho \mathbf{b} \cdot \mathbf{v}^h \, d\Omega + \int_{\Gamma_h} \mathbf{t}_h \cdot \mathbf{v}^h \, d\Gamma + \sum_{K \in \Omega^h} \int_{\Omega_K} \rho \mathbf{b} \cdot \alpha (\nabla q^h - \operatorname{div} \mathbf{S}^h) \, d\Omega \tag{5}$$

with $\boldsymbol{\Sigma}^h \times P^h \times \mathbf{V}_g^h$ *is the finite element product sub-space for extra-stress, pressure and velocity, respectively, and the stability parameter* $\alpha(Re_K)$ *and* $\beta(De_K)$*, are extensions of the stability parameter introduced by Franca and Frey (1992) for approximations of constant viscosity fluid flows.*

3. NUMERICAL RESULTS

In this section, the multi-field GLS formulation (Eq.(3)-(5)) is used to approximate upper-convected Maxwell fluid flows defined by Eq.(1)-(2). The geometry and flow kinematics are depicted in Fig. 1a, for a coordinate Cartesian system with origin on the cylinder center. The channel aspect ratio is defined as the half height of the channel (h) divided by the cylinder radius (R) - with h/R=8 as suggested in (Behr et al., 2004). Due to flow domain symmetry, only half the channel is used in the numerical computations. After a mesh independence test on the dimensionless pressure coefficient, $p^* = p/\rho U^2$, the computational domain Ω^h is partitioned into an equal-order combination of 2,860 Lagrangian bi-linear (Q1) finite elements for extra-stress, pressure and velocity fields. Fig. 1b shows a blow-up view of the chosen mesh around the cylinder.

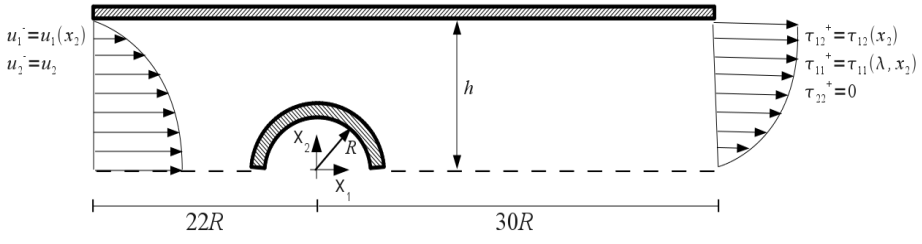

(a)

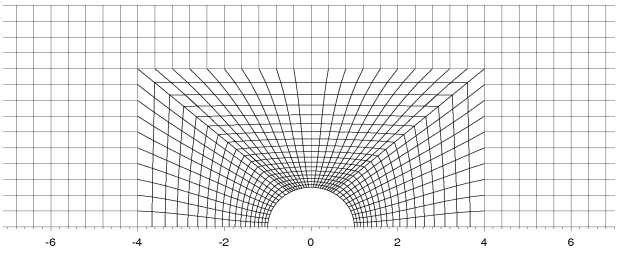

(b)

Figure 1. Flow around a confined cylinder: (a) the problem statement; (b) a mesh detail.

The boundary conditions are (i) no-slip and impermeability on channel walls and cylinder surface, (ii) velocity and extra-stress symmetry conditions on the centerline, and (iii) fully-developed velocity and extra-stress profiles at inflow and outflow. The Deborah number, here defined in terms of the average inlet velocity U and the cylinder radius R, is expressed by

$$De=\frac{\lambda U}{R} \tag{6}$$

where λ is the relaxation time.

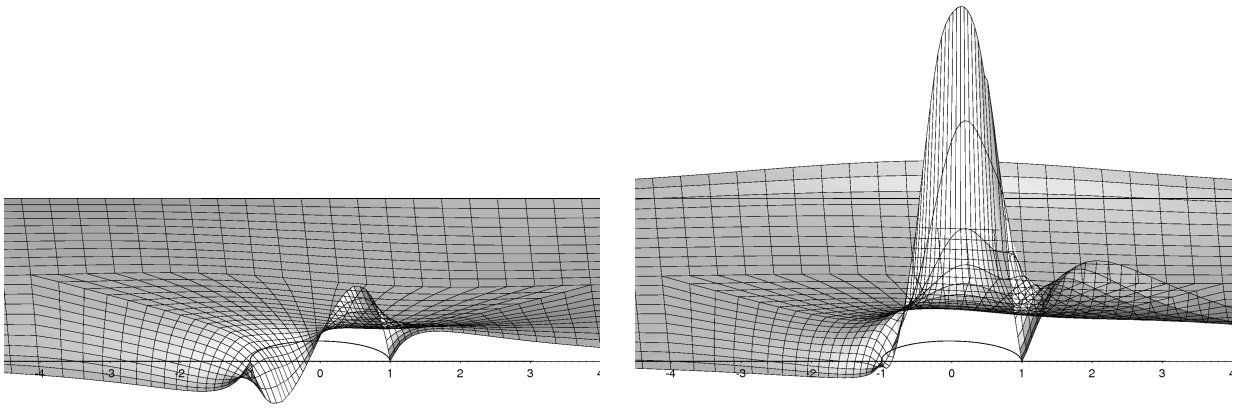

(a) (b)

Figure 2. τ_{11}^* elations plots around the cylinder, for Re=0: (a) De=0; (b) De=0.9.

Figures 2 and 3 show extra-stress elevation plots around the cylinder, for creeping flow (Re=0). Fig. 2 shows the dimensionless normal stress profiles, $\tau_{11}^*=\tau_{11}R/\eta_p U$, for De=0-0.9, while Fig. 3a-3b present dimensionless normal stress profiles, $\tau_{22}^*=\tau_{22}R/\eta_p U$, and shear stress profiles, $\tau_{12}^*=\tau_{12}R/\eta_p U$, respectively, for De=0.9. It can be observed that τ_{11} is symmetric around the cylinder for the Newtonian case - De=0 (Fig. 2a), which is in accordance to the typical behavior for inelastic fluids. This symmetry is broken as Deborah increases (Fig. 2b), with the maximum τ_{11}^* reaching a value much higher than the Newtonian one . Besides, this maximum normal axial traction begins to occur just before the cylinder equator, certainly due to the fluid extension induced by the area restriction.

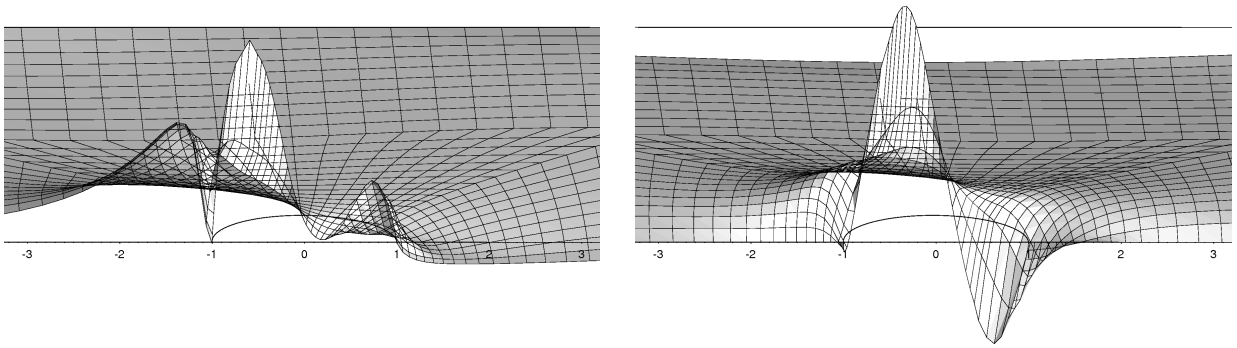

(a) (b)

Figure 3. (a) τ_{22}^* and (b) τ_{12}^* elevations around the cylinder, for Re=0 and De=0.9.

From Fig. 3a-3b, it can be noticed that τ_{22}^* and τ_{12}^* levels also increase with elasticity. Moreover, the maximum values of both extra-stress fields occur in the inflow surface of the cylinder, probably due to the locally extensional kinematics imposed by the cylinder, leading to higher values of the strain-rates. The τ_{22}^* normal component presents two peaks just upstream of the cylinder (Fig. 3a) and the shear component τ_{12}^* presents a greater value accelerating the fluid, in the inflow surface, than the value retarding it, in the outflow (Fig. 3b).

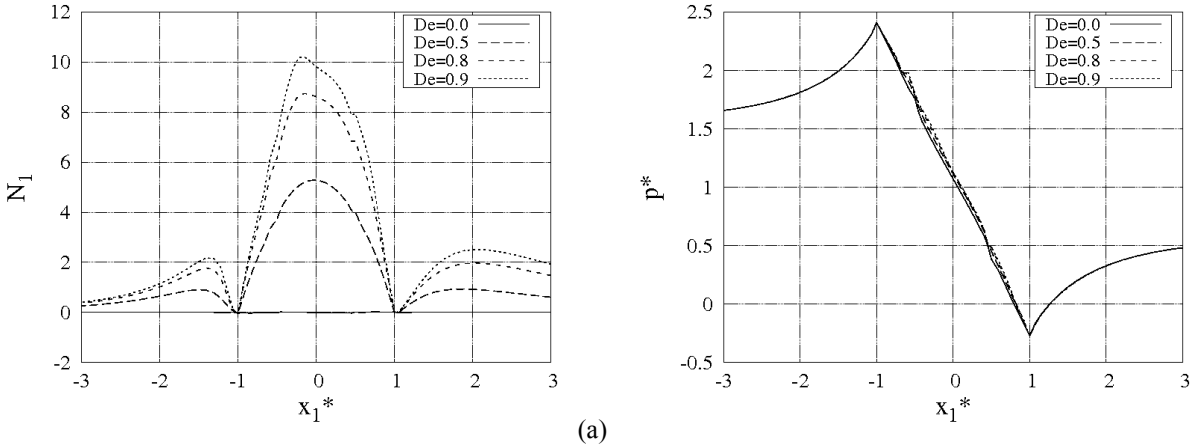

(a) (b)

Figure 4. Longitudinal first normal stress difference and pressure profiles at x_2^*=0, for Re=0, De=0-0.9: (a) N_1; (b) p^*.

In order to complement and quantify the analysis introduced in Figs. 2 and 3, the first normal stress, $N_1 = \tau_{11}^* - \tau_{22}^*$, and pressure profiles are presented in Fig. 4a and 4b, in which the dimensionless coordinates $x_1^* = x_1/R$ and $x_2^* = x_2/R$. For the inelastic case (De=0), a null first normal stress difference is obtained, as expected (Fig. 4a). Increasing the Deborah number, the first normal stress difference changes from zero to around 10 (Fig. 4a, for De=0 -0.9) close to the cylinder wall. While the extra-stress are stronger dependent on De, the pressure field seems to be unaffected by fluid elasticity, since it presents only some local slight disagreement for De=0.9 (Fig. 4b), probably due to some numerical oscillations.

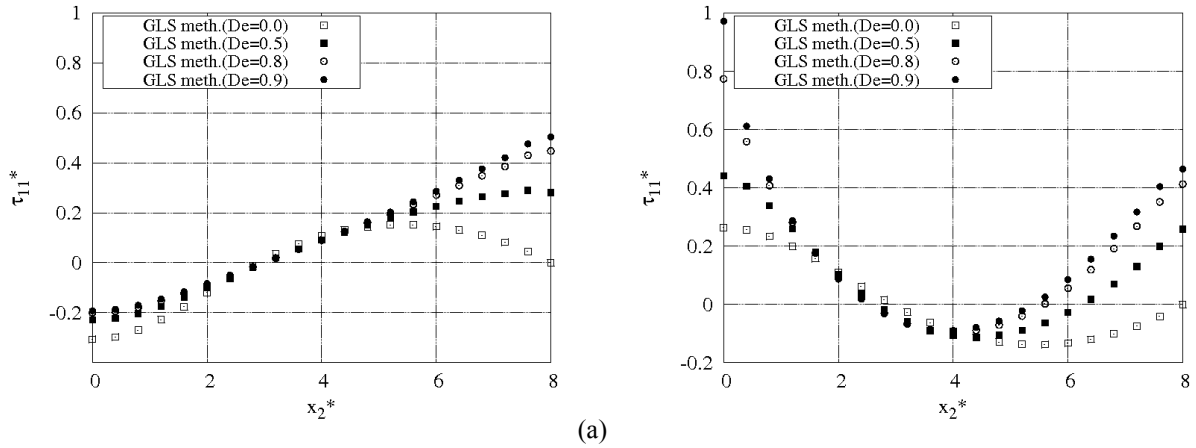

(a) (b)

Figure 5. τ_{11}^* transverse profiles for Re=0 and De=0-0.9: (a) x_1^*= -5; (c) x_1^*= +5

Finally, the influence of the stress advective term of the UCM equation (Eq.(1)-(2)) on the flow pattern is investigated in Fig. 5. The τ_{11}^* profiles present an axisymmetric pattern around the cylinder, as illustrated by Fig. 5a and 5b. Note that, despite both profiles have been evaluated at equal distance from the origin (at x_1^*=-5, in Fig. 5a, and x_1^*=+5, in Fig. 5b), the influence of the cylinder is stronger downstream than upstream. This axisymmetric flow pattern is typically verified in advective dominated viscous flows. However, since inertia is neglected in Eq. (1), this behavior should be due to the stress advective term present in the material equation.

4. FINAL REMARKS

In this work a multi-field GLS approximation for upper-convected Maxwell model is used to analyze the creeping flow around a cylinder between two parallel plates, for the Deborah number varied from 0 to 0.9. The numerical results

confirmed the good stability features of the multi-field GLS formulation for elastic-dominated flows, using a combination of quadrilateral bi-linear finite elements. For purely dissipative flows (De=0), the extra-stress profiles for creeping flows show a symmetry, which is broken by fluid elasticity. Moreover, much higher values of the extra-stress close to the cylinder are obtained, as the elasticity increases.

5. ACKNOWLEDGEMENTS

The author C. Fonseca thanks for his graduate scholarship provided by CAPES and the authors S. Frey and M. Naccache acknowledges CNPq for financial support.

6. REFERENCES

Astarita, G. Marrucci, G., 1974, "Principles of Non-Newtonian Fluid Mechanics". McGraw-Hill, Great Britain.

Behr, M., Coronado, O. M., Arora, D. and Pasquali, M., 2004, "Stabilized Finite Element Methods of GLS type for Oldroyd-B Viscoelastic Fluid ". European Congress on Comput. Methods in Appl. Sciences. and Engrg. - ECCOMAS 2004.

Behr, M., Franca, L.P., Tezduyar, T.E., 1993. "Stabilized Finite Element Methods for the Velocity-Pressure-Stress Formulation of Incompressible Flows", Comput. Methods Appl. Mech. Engrg., Vol. 104, pp. 31-48.

Franca, L. P., Frey, S., 1992, "Stabilized Finite Element Methods: II. The Incompressible Navier-Stokes Equations". Computer Methods in Applied Mechanics and Engineering, 99, pp. 209-233.

Owens, R. G. and Phillips, T. N., 2002, "Computational Rheology", Imperial College Press, London, UK.

7. RESPONSIBILITY NOTICE

The authors are the only responsible for the printed material included in this paper.